Microfluid Nanofluid (2014) 16:605–612
DOI 10.1007/s10404-013-1250-5

BRIEF COMMUNICATION

Isolation and elution of Hep3B circulating tumor cells using a dual-functional herringbone chip

Peng Xue · Kai Ye · Jie Gao · Yafeng Wu · Jinhong Guo · Kam M. Hui · Yuejun Kang

Received: 7 May 2013 / Accepted: 12 August 2013 / Published online: 24 August 2013
© Springer-Verlag Berlin Heidelberg 2013

Abstract Circulating tumor cells (CTCs), which are derived from primary tumor and circulate to secondary site, are regarded as the cause of metastasis. Many methods have been applied for CTC isolation and enumeration so far. However, it remains a challenge to effectively elute the captured cells from the device for further cellular and biomolecular analyses. In this paper, we fabricate a dual-functional herringbone chip to achieve both CTC capture and elution based on the immunoassay of epithelial cell adhesion molecule antigen expressed on the surface of human liver cancer cell line Hep3B. The results show that the capture limit of Hep3B cells can reach as low as 3 cells per ml with capture efficiency over 50 % on average. On the other hand, the elution rate of more than 50 % of the captured Hep3B cells can be achieved for cell density ranging from 5 to 2×10^3/ml. It demonstrates that this herringbone chip exhibits excellent dual functions with high capture efficiency and considerable elution rate, indicating its promising capability for clinical assay in cancer diagnosis.

Keywords Circulating tumor cells · Hep3B · EpCAM · Cell capture · Cell elution

P. Xue · Y. Wu · J. Guo · Y. Kang (✉)
School of Chemical and Biomedical Engineering, Nanyang Technological University, 62 Nanyang Drive, Singapore 637459, Singapore
e-mail: yuejun.kang@ntu.edu.sg

K. Ye · J. Gao · K. M. Hui (✉)
Division of Cellular and Molecular Research, National Cancer Centre, 11 Hospital Drive, Singapore 169610, Singapore
e-mail: cmrhkm@nccs.com.sg

1 Introduction

Circulating tumor cells are derived from primary tumor site and transported to distant organs through circulatory blood system, which is known to cause metastatic cancer (Zetter 1998). The characterization of the CTCs is critical to evaluate the treatment efficacy and monitor disease progression due to the fact that the number of the CTCs in peripheral blood is proportionally correlated to the extent of metastases (Hsieh et al. 2006; Kim and Jung 2010; Stott et al. 2010a, b; Hou et al. 2012). The isolation and enumeration of CTCs is highly challenging, however, due to the extremely low cell density, normally 1–10 CTCs per ml of blood in cancer patients (den Toonder 2011). The devices based on microfluidic technique have many advantages, such as tiny sample volume, high throughput, fast processing, and multifunctional detection, which provides the opportunity for rapid and efficient CTC detection and characterization for point-of-care applications (van de Stolpe et al. 2011). The large surface-to-volume ratio of the microdevices further facilitates reliable cell capturing using complex microfluidic patterning. Cell-affinity chromatography (Nagrath et al. 2007; Stott et al. 2010a, b), immunomagnetic cell capture (Hoshino et al. 2011; Kang et al. 2012), size-based cell capture (Hur et al. 2011; Zheng et al. 2011), and dielectrophoretic (DEP) (Becker et al. 1995) methods have been commonly applied for CTC detection and isolation.

In 2010, an enhanced microfluidic mixing device was developed using a unique herringbone structure, which increased the interaction between the modified chip surface and the target human prostate cancer cells (PC3) based on cell-affinity chromatography (Stott et al. 2010a, b). This 3D herringbone design significantly enhanced the mixing within each groove and facilitated cancer cell capture. For

CTC concentration of 1,000/ml, they reported capture rates that ranged from 40 % under higher flow rate (0.48 ml/h) to 80 % under lower flow rate (0.12 ml/h). As a clinical trial using their device, CTCs were detected in 14 among the 15 patients who have prostate cancer at metastatic stage (386 ± 238 CTCs/ml). Although these devices have been applied for efficient CTC capture and enumeration, most of them can only realize the major function solely for cell capture. However, the bound CTCs usually cannot be reversibly released after capture due to the strong interaction between antigen and antibody. For clinical application, there exists an urgent need for harvesting the captured CTCs for further analyses, such as enzyme-linked immunosorbent assay (ELISA), polymerase chain reaction (PCR), cytometric, and electrochemical techniques (Arya et al. 2013), which cannot be easily achieved in situ. These cellular and biomolecular characterizations of CTCs are essential for confirmation and in-depth understanding of the metastasis process, based on which medical diagnosis and treatment can be made to suppress the progression of tumor disease (Kim et al. 2009; Sieuwerts and Jeffery 2012). For this purpose, several common methodologies as mentioned above have shown some potential for on-chip cell elution and harvesting. For instance, the dielectrophoretic separation method can purify and elute the captured CTCs by simply adjusting the applied electric field (Becker et al. 1995). However, this electrical method usually suffers from many negative effects on the cell physiology due to the imposed membrane stress, Joule heating, and thermal decomposition (Voldman 2006; Kang and Li 2009). As another example, the immunomagnetic CTC detection method assisted by anti-EpCAM-coated nanoparticles can realize cell elution and harvesting by removing the magnetic field (Hoshino et al. 2011; Kang et al. 2012). Nonetheless, there is no report on how these conjugated nanoparticles would affect the cell physiology and subsequent molecular analysis, neither on how to remove the magnetic particles from the cell membrane after elution.

Therefore, a dual-functional chip is desired to enable the cell elution successively after capturing CTCs. In this paper, for the first time, a dual-functional herringbone chip is developed for Hep3B cell capture and elution. Hep3B is a typical hepatocellular carcinoma cell line and its number density in patients' blood is essential for determining hepatocellular carcinoma metastasis stage. The herringbone chip was fabricated by using PDMS elastomer, and the surface of the inner channel wall was modified with anti-EpCAM based on a previous report (Stott et al. 2010a, b). Subsequently, Hep3B cells were spiked into PBS and whole blood, respectively, before being introduced into the microchip by a syringe pump. The capture rate was calculated by using the fluorescent microscopy after immunoreaction. D-biotin was then introduced into the microchannel to displace the site of biotinylated anti-EpCAM conjugation, followed by the elution of unbound cells from the device (Hirsch et al. 2002). In this paper, we found that the capture rate for CTCs spiked into whole blood at the density of 2,000/ml and 400/ml could reach 53 % for perfusion rate of 1 ml/h, which is comparable to that obtained in the previous work (Stott et al. 2010a, b). In addition, we also investigated the CTC capture capability of this device under a wide dynamic range of the cell number density in the sample. In particular, we achieved acceptable capture rates for extremely low CTC concentrations of 100/ml, 40/ml, and 3/ml, respectively, which are much more clinically relevant cell densities for early diagnosis of cancer and have not been reported by the previous literature. More importantly, we have studied the elution rates under different CTC concentrations. The elution function based on the D-biotin-assisted competitive inhibition is a unique feature of this approach, and there is no previous report of similar study on CTC elution so far. The present CTC chip can achieve over 50 % for both capture rate and elution rate, demonstrating its potential applications in clinical assay for cancer diagnostics.

2 Experimental methods

2.1 Design of the herringbone chip

The chip is composed of one common inlet, one common outlet, and eight herringbone structure channels. The height of the herringbone structures is 45 μm; height of channel space below herringbone structure is 50 μm; and the width of chevron pattern is 50 μm. Gap between the neighbor herringbones is 50 μm. The angle between the herringbone and the channel longitudinal axis is 45°. The herringbone grooves are patterned in alternate permutation to induce chaotic mixing and increase the total surface area to enhance rare cell capture from the sample. The mold was fabricated on a silicon wafer and the chip design is shown in Fig. 1.

2.2 Chip fabrication

SU-8-negative photoresist was patterned on the silicon wafer to create a 3D mold including negative herringbone structure and flow channel using photolithography. PDMS microchannels are fabricated by rapid prototyping using the above-mentioned mold with elastomer base and elastomer curing agent mixed at the ratio of 10:1 (Ng et al. 2002). The final chip was integrated by bonding the PDMS slice and a $1'' \times 3''$ glass slide together after plasma treatment.

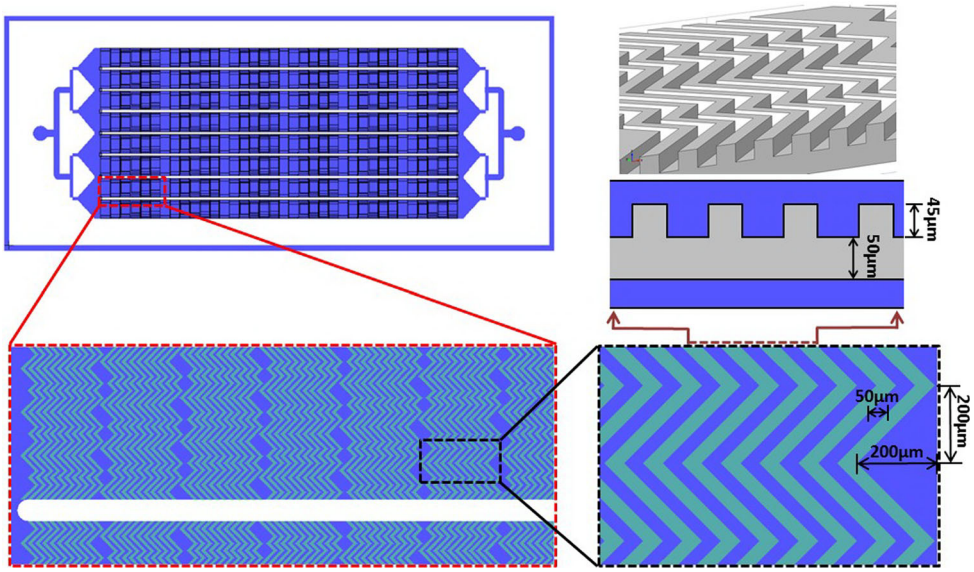

Fig. 1 Schematic design of the microfluidic chip with three-dimensional geometry of the herringbone channels and their dimensions in horizontal and vertical cross-sections

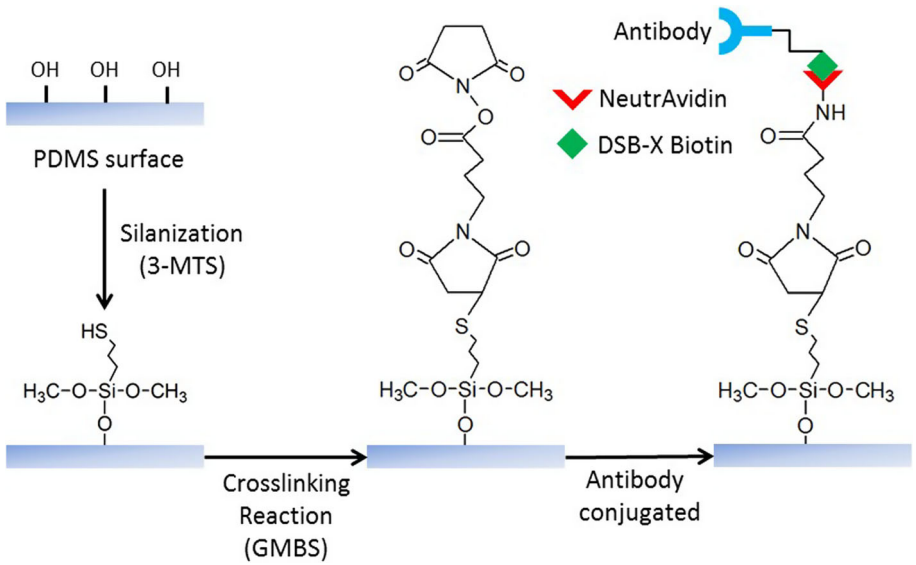

Fig. 2 Procedure of antibody immobilization on PDMS surface

2.3 Channel surface modification with anti-EpCAM

The microchannels were treated with 4 % (v/v) 3-MPTS (3-mercaptopropyl trimethoxysilane) in ethanol at room temperature immediately after chip fabrication. The chip was washed with ethanol thoroughly, followed by incubation with 10 mM GMBS (N-y-maleimidobutyryloxy succinimide ester) for 30 min in ambient environment. The chip was eluted with PBS (pH = 7.4) thoroughly and then treated with 10 μg/ml NeutrAvidin biotin-binding protein in PBS for 30 min at room temperature. Subsequently, the chip was incubated with 20 μg/ml biotinylated antihuman EpCAM (with 1 % BSA) for 30 min at room temperature. Then, the chip was washed with PBS thoroughly and ready for use. The procedure on immobilization of anti-EpCAM is shown in Fig. 2.

2.4 Hep3B CTC capture test

The setup includes three components: a syringe pump unit, a microchip core unit, and a waste collection unit. The number density of Hep3B cells was counted with a hemocytometer and stained with fluorescent dye CFDA-SE, and spiked into 1 ml of PBS or whole blood from healthy donors. Then, the sample was introduced into the prepared microchip at a flow rate of 1 ml/h precisely controlled by a syringe pump for 1 h, followed by rinsing with PBS buffer (pH = 7.4) at a flow rate of 4 ml/h to remove

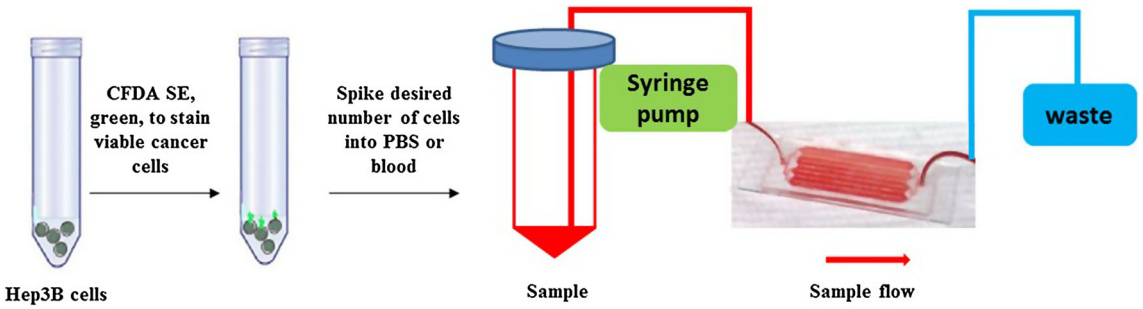

Fig. 3 Illustration of CTC capture process

the unbound Hep3B cells and other blood cells from the chip. The number of captured cells was counted under a fluorescent microscope and capture rate was calculated accordingly. The overall process is illustrated in Fig. 3.

2.5 Hep3B CTC elution test

For elution test, 10 mM of D-biotin was introduced into the microchannels to block the binding sites of EpCAM antibody. After incubation for 30 min, the chip was washed with PBS manually for three times by simply using a pipette to remove the released Hep3B cells. The elution rate is calculated based on the ratio between the total number of the bound cells after and before the elution.

3 Results and discussion

3.1 Chip fabrication and flow simulation studies

Since it is very challenging to directly measure the flow velocity inside the microchip, a finite element-based numerical simulation was conducted to estimate and characterize the flow condition by using COMSOL Multiphysics 4.2a (COMSOL, CA, USA). The detailed numerical model and the boundary conditions for the simulation were defined as follows.

Since the flow is pressure driven only, the steady-state Navier–Stokes equation for incompressible flow is shown as:

$$\rho(\vec{u}\cdot\nabla\vec{u}) = -\nabla p + \eta\nabla^2\vec{u} \quad (1)$$

Continuity equation:

$$\nabla\vec{u} = 0 \quad (2)$$

Boundary conditions:

$$\text{Channel walls: } \vec{u} = 0,\ \vec{n}\cdot\nabla p = 0 \quad (3a)$$

$$\text{Inlet: } v = 76\,\mu\text{m/s} \quad (3b)$$

$$\text{Outlet: } p = 0 \quad (3c)$$

where $\vec{u}$ is flow velocity; p is the pressure; η is the fluid viscosity; ρ is the fluid density.

One typical section of the microchannel with 2-mm-long herringbone structure (Fig. 4a) was simulated for discrete streamlines (Fig. 4b) and flow velocity (Fig. 4c). The inflow velocity was set as 76 μm/s (corresponding to the actual perfusion rate of 1 ml/h). From the simulation results in Fig. 4b, c, a very unique flow pattern can be observed that the herringbone structures on the channel ceiling split part of the main channel flow into the grooves periodically and recombine them with main flow at the end of the herringbone structure. Thus, the cell-laden flow has a much larger interface area with the antibody-functionalized groove wall, where the average flow speed is 17 μm/s compared to that of 118 μm/s in the main channel as shown in Fig. 4c. The flow inside the herringbone grooves is much slower than the main channel flow, which is highly favorable for the immunological interaction between the CTCs and the antibody-functionalized channel wall. In addition, from the 3D streamlines in Fig. 4, the groove flow direction has been deviated by 45° compared to the main channel flow, which effectively increases the total flow distance in the herringbone structure. The combination of these three features, such as flow splitting for large interface area, slower groove flow, and longer flow distance, significantly contributes to the enhanced immunoreaction between the cell surface ligand and the immobilized antibody and thus the tumor cell binding in the herringbone structure. Therefore, this herringbone chip is inherently much more advantageous than other chip designs with bare straight channels, leading to a much higher capture rate of the CTCs.

However, the elution of CTCs is mainly dependent on the diffusion of biotin and the competitive surface reaction between the biotin and the antibody to block the binding sites for CTCs. The above three flow features that enhance cell capture do not contribute to promoting the diffusion of biotin or its surface reaction. Biotin is water-soluble organic compound with molecular weight of about 244, which is much smaller than biological cells such as CTCs.

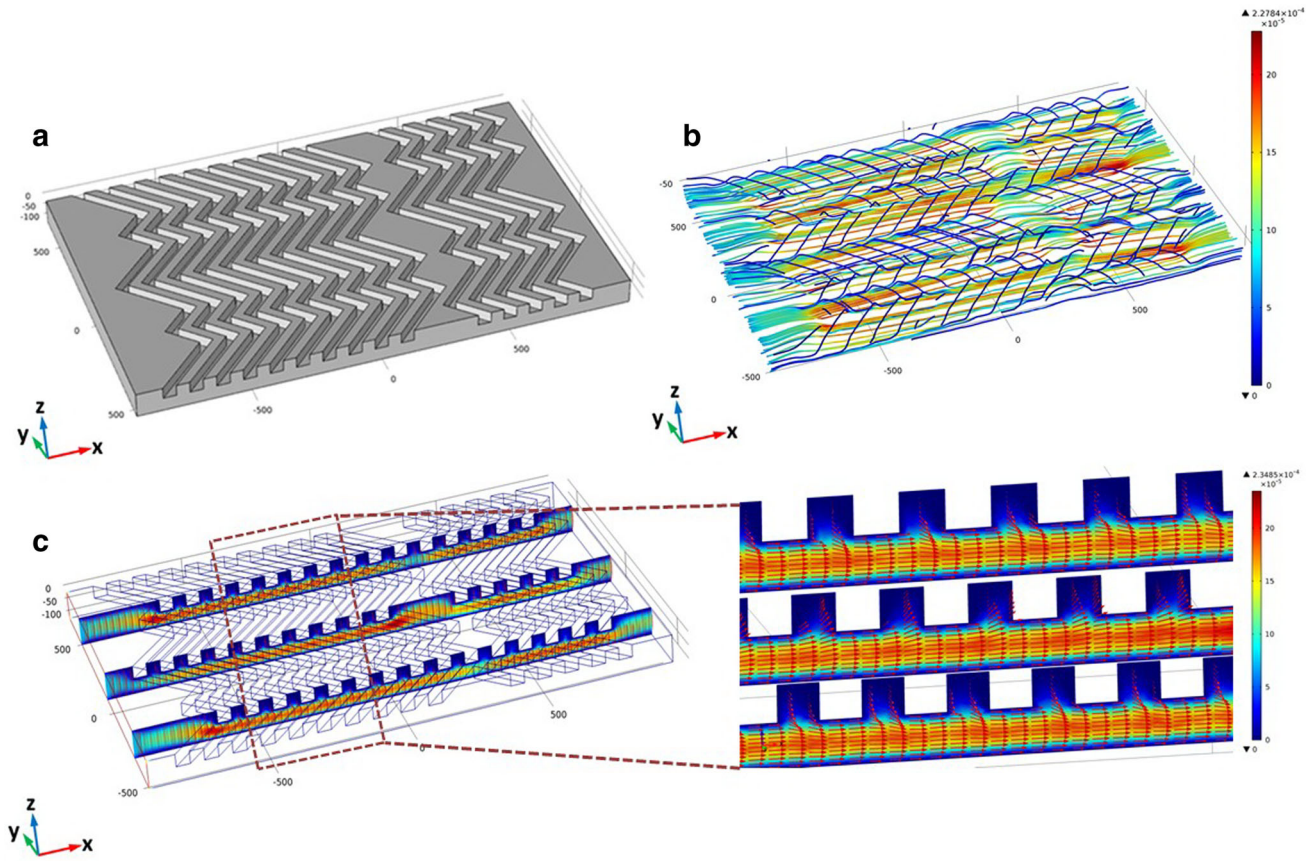

Fig. 4 Numerical simulation of the liquid flow in a herringbone chip: **a** three-dimensional view of the channel geometry for computation with profile of herringbone structure; **b** three-dimensional view of the simulated flow streamline, which occurs in the corresponding domain as shown in **a**; **c** two-dimensional cross-sectional view (in ZOX plane) of the simulated velocity field at three different locations

Therefore, the diffusion rate of biotin molecules is much greater than that of biological cells, which implies that the limiting factor for enhancing the competitive surface reaction is the surface area. Meanwhile, the herringbone chip is characterized by a large number of microgrooves, which effectively increases the total surface area for the reaction between dissolved biotin and the immobilized antibody on the channel wall. After introducing the biotin as a competitor to active cell binding sites, the captured cells can be rapidly disassociated from the channel wall and the elution process can be simply achieved by washing with PBS. In this respect, the unique herringbone structure also helps the CTC elution, however, due to a totally different mechanism compared with cell capture.

3.2 Capture and elution study of Hep3B CTCs spiked in PBS

CFDA-SE is a fluorescent tracer for long-term cell labeling. Green fluorescence can be observed after cell staining under fluorescence microscope. CFDA-SE diffuses into cells and forms an amine-reactive compound. This product generates an observable fluorescence and binds to intracellular amine sources. This dye is advantageous in that local concentration of 10 μM is sufficient for staining with minimum cell death. After introducing the PBS spiked with 10^4 CTCs into the chip, microscopic images of the captured CTCs under both bright field and dark field were taken as shown in Fig. 5a, b. The number of remaining bound cells after elution can be counted under fluorescent microscope through CFDA-SE staining as shown in Fig. 5d. It is obvious that the Hep3B cells were successfully captured in the herringbone structure and green fluorescent dots in the dark field represent captured live tumor cells locating at the same position as the ones in the bright field. The capture efficiency and elution rate can be calculated by comparing the number of bound CTCs before and after elution with the total number of spiked CTCs.

The capture rates of CTCs spiked into PBS with different number density are demonstrated in Fig. 6, which shows an average capture rate of more than 50 % for the cell density ranging from 3 to 10^4/ml. It was also noticed that, for the cell density of 10^5/ml, the capture rate reduced to only 9.5 %, which is due to the saturation of the binding

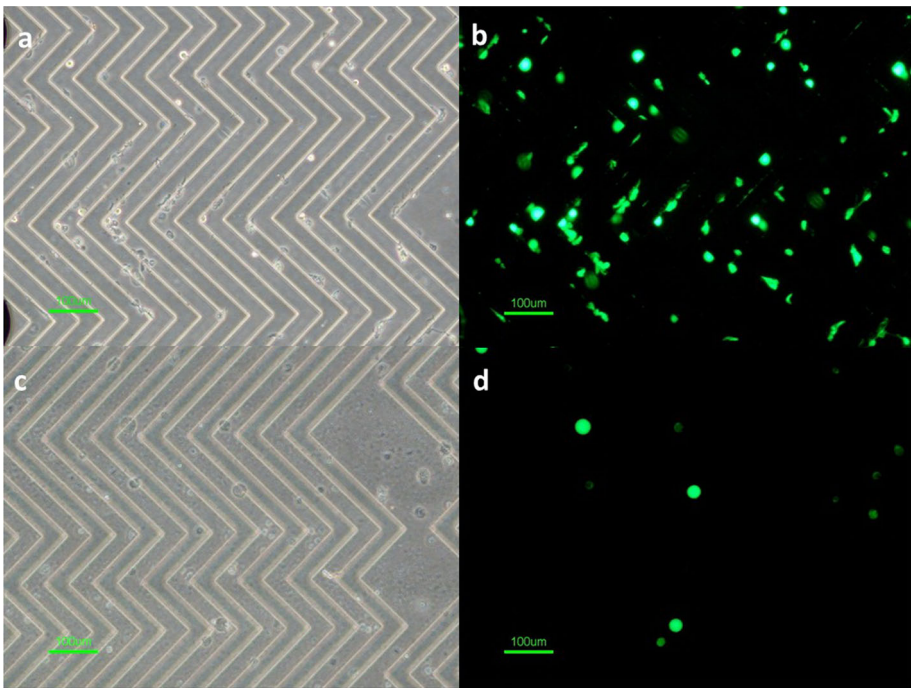

Fig. 5 Microscopic images of captured CTCs before elution under bright field (**a**) and dark field (**b**); the remaining bound CTCs after elution under bright field (**c**) and dark field (**d**). (*Scale bar*: 100 μm)

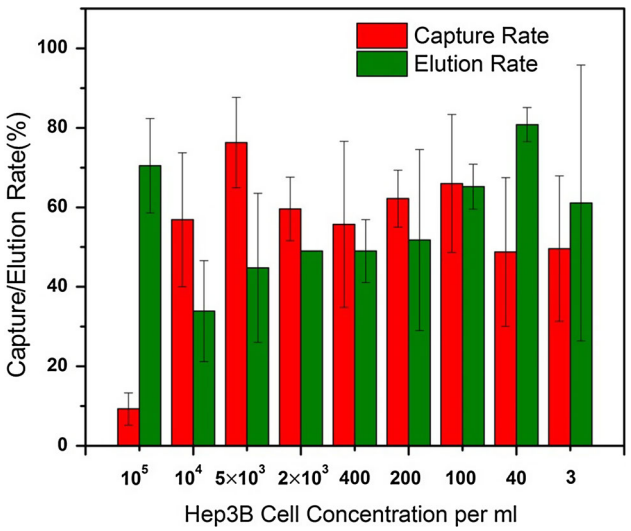

Fig. 6 Capture and elution rates of CTCs spiked in PBS in different cell number density

sites between the immobilized antibodies and the tumor cells. This implies that the total number of the tumor cells perfused through the chip significantly exceeded the number of immobilized antibodies and hence depleted all the binding sites for extra cell capture. Nonetheless, 10^5 CTCs per ml is far from the realistic density of clinical samples anyway, while this result can still reveal important information for quantifying the active binding sites of the immobilized antibodies on a particular chip. On the other hand, for the more clinically relevant cell density of 3 and 40/ml, the effective capture rate can reach 48.8 and 49.6 %, respectively, which is an acceptable level for the isolation of extremely rare cells like CTCs. In addition, the lowest detection limit achieved by this device was 3 CTCs per ml, which is sufficiently sensitive for clinical applications. The measured capture rates are comparable to the previous report (Stott et al. 2010a, b), and the results are consistent for five repeated tests for each cell density. The results indicated that the herringbone chip coated with anti-EpCAM has significantly enhanced cell capture efficiency based on the interaction between the antibody-coated channel wall and the biomarker expressed on cancer cell surface. It is further proved that the microchannel fabricated based on herringbone structure has 3–4 times higher capture rate than the traditional flat channel (Stott et al. 2010a, b). The overall processing time for 1 ml of sample takes only 1 h, which is considerably rapid for clinical applications.

For harvesting the captured CTCs, D-biotin is introduced and will compete with the active reaction sites on NeutrAvidin that are originally bounded with anti-EpCAM. This competitive inhibition will deactivate the capture antibody and result in captured tumor cells being disassociated from the channel wall. The test results showed a high elution rate of more than 50 % on average with the sample cell density from 3 to 10^5/ml. For the more clinically relevant cell number density of 3 and 40/ml, the elution rates reached up to 61.1 and 80.8 %, respectively, which demonstrated a significant effect of D-biotin on antibody blockage. In a control experiment, we also tried cell elution solely by PBS washing without the application of D-biotin. It was observed that only using PBS washing

could not effectively elute the captured CTCs and the elution rate was as low as 1 % for density of 1,000 CTCs/ml. Therefore, it is the biotin-induced cell disassociation, rather than the flow-induced shear stress that enables the captured cells to be eluted from the chip. This excellent feature can be utilized for eluting and harvesting isolated CTCs efficiently from the chip for subsequent cellular and biomolecular analyses on cancer progression.

3.3 Capture and elution study of Hep3B CTCs spiked in whole blood

In order to evaluate the device performance on actual human blood, different numbers of CTCs were spiked into fresh whole blood samples from healthy donors and were tested for CTCs capture and elution using the developed chips. Compared to the previous results done with CTCs spiked into PBS, the same device demonstrated a similar CTC capture rate of more than 50 % on average with the cell number density from 5 to 2 × 10^3/ml of blood, as shown in Fig. 7. With respect to more clinically relevant Hep3B number density of 5 and 30/ml of blood, the effective capture rate could reach up to 50 and 83.3 %, respectively. For the error bars going beyond 100 %, those are attributed to the slight errors in spiking concentration of tumor cells, it indicated that this herringbone chip was also capable of processing whole blood sample with a high capture rate. Even under the shear stress generated by the flow of 4 ml/h PBS rinsing buffer, the interaction between the antibody and Hep3B was still strong enough to ensure the stable binding of the captured CTCs during washing process. On the other hand, the highly complex background in the circulating blood, such as erythrocytes, leukocytes, platelets, and other nontarget cells, did not show obvious nonspecific binding on the herringbone structure due to the weak expression of EpCAM on their membranes. Therefore, the herringbone structure modified by EpCAM antibody can specifically capture tumor cells without the inference from other cell types. After introducing D-biotin, the captured tumor cells were successfully disassociated from the channel wall with elution rate of more than 50 % on average. For the CTC number density of 30 and 5/ml of blood, the elution rate can be achieved as 54 and 75 %, respectively.

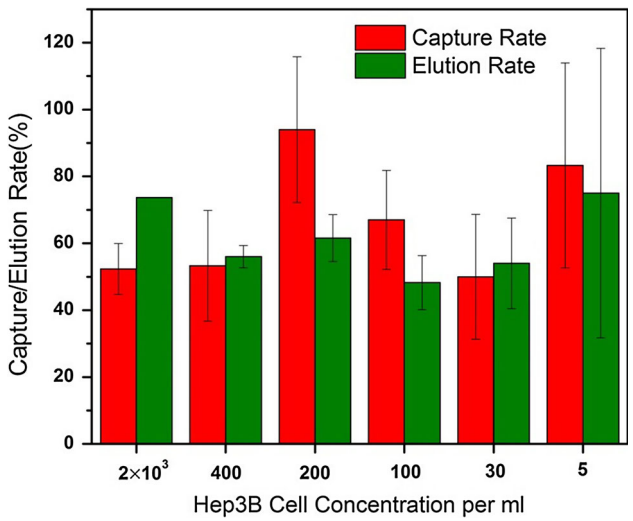

Fig. 7 Capture and elution rates of CTCs spiked in whole blood in different cell number density. Due to the human errors in spiking CTC concentration, the actual spiked cell number could be higher than the nominal value, which would lead to a capture/elution rate above 100 % as shown in some of the *error bars*

4 Conclusions

A dual-functional herringbone microfluidic chip was fabricated and utilized for capture and elution of Hep3B CTCs from PBS and whole blood samples. DSB-X biotinylated Anti-EpCAM was covalently coated on the internal channel of this microdevice for CTCs capture. For elution process, D-biotin was introduced to block the antibody reaction site based on higher affinity of D-biotin binding to NeutrAvidin. The number of the captured cells and eluted cells was counted under fluorescent microscope. The capture rate for Hep3B spiked in PBS, and whole blood tested on this chip is comparable to the previous report. Moreover, in a detailed study on CTC harvesting, the captured Hep3B can be successfully eluted from the chip with an outstanding elution rate. More specifically, capture and elution rate of Hep3B was studied for a wide dynamic range of the CTC number density in the sample. The presented dual-functional device showed ultrahigh sensitivity and specificity to capture and elute Hep3B CTCs with excellent reproducibility and stability, indicating its enabling capability for applications in cancer diagnostics.

Acknowledgments This work was supported by a start-up grant from Nanyang Technological University College of Engineering, a Tier-1 Academic Research Fund from the Ministry of Education of Singapore (RG 26/11) awarded to Y.J.K., and research grants from the SingHealth Foundation, the Singapore National Medical Research Council, the Biomedical Research Council of Singapore, and the Singapore Millennium Foundation awarded to K.M.H.

Conflict of interest The authors declare no conflict of interest.

References

Arya SK, Lim B, Rahman AR (2013) Enrichment, detection and clinical significance of circulating tumor cells. Lab Chip 13(11):1995–2027. doi:10.1039/c3lc00009e

Becker FF, Wang XB, Huang Y, Pethig R, Vykoukal J, Gascoyne PR (1995) Separation of human breast-cancer cells from blood by differential dielectric affinity. Proc Natl Acad Sci USA 92(3):860–864. doi:10.1073/pnas.92.3.860

den Toonder J (2011) Circulating tumor cells: the grand challenge. Lab Chip 11(3):375–377. doi:10.1039/c0lc90100h

Hirsch JD, Eslamizar L, Filanoski BJ, Malekzadeh N, Haugland RP, Beechem JM, Haugland RP (2002) Easily reversible desthiobiotin binding to streptavidin, avidin, and other biotin-binding proteins: uses for protein labeling, detection, and isolation. Anal Biochem 308(2):343–357. doi:10.1016/S0003-2697(02)00201-4

Hoshino K, Huang YY, Lane N, Huebschman M, Uhr JW, Frenkel EP, Zhang X (2011) Microchip-based immunomagnetic detection of circulating tumor cells. Lab Chip 11(20):3449–3457. doi:10.1039/c1lc20270g

Hou L, Zhang X, Gawron AJ, Liu J (2012) Surrogate tissue telomere length and cancer risk: shorter or longer? Cancer Lett 319(2): 130–135. doi:10.1016/j.canlet.2012.01.028

Hsieh HB, Marrinucci D, Bethel K, Curry DN, Humphrey M, Krivacic RT, Kroener J, Kroener L, Ladanyi A, Lazarus N, Kuhn P, Bruce RH, Nieva J (2006) High speed detection of circulating tumor cells. Biosens Bioelectron 21(10):1893–1899. doi:10.1016/j.bios.2005.12.024

Hur SC, Mach AJ, Di Carlo D (2011) High-throughput size-based rare cell enrichment using microscale vortices. Biomicrofluidics 5(2):022206. doi:10.1063/1.3576780

Kang Y, Li D (2009) Electrokinetic motion of particles and cells in microchannels. Microfluid Nanofluid 6:431–460. doi:10.1007/s10404-009-0408-7

Kang JH, Krause S, Tobin H, Mammoto A, Kanapathipillai M, Ingber DE (2012) A combined micromagnetic-microfluidic device for rapid capture and culture of rare circulating tumor cells. Lab Chip 12(12):2175–2181. doi:10.1039/c2lc40072c

Kim SI, Jung HI (2010) Circulating tumor cells: detection methods and potential clinical application in breast cancer. J Breast Cancer 13(2):125–131. doi:10.4048/jbc.2010.13.2.125

Kim MY, Oskarsson T, Acharyya S, Nguyen DX, Zhang XH, Norton L, Massagué J (2009) Tumor self-seeding by circulating cancer cells. Cell 139(7):1315–1326. doi:10.1016/j.cell.2009.11.025

Nagrath S, Sequist LV, Maheswaran S, Bell DW, Irimia D, Ulkus L, Smith MR, Kwak EL, Digumarthy S, Muzikansky A, Ryan P, Balis UJ, Tompkins RG, Haber DA, Toner M (2007) Isolation of rare circulating tumour cells in cancer patients by microchip technology. Nature 450(7173):1235–1239. doi:10.1038/nature06385

Ng JM, Gitlin I, Stroock AD, Whitesides GM (2002) Components for integrated poly (dimethylsiloxane) microfluidic systems. Electrophoresis 23(20):3461–3473. doi:10.1002/1522-2683(200210)23:20<3461:AID-ELPS3461>3.0.CO;2-8

Sieuwerts AM, Jeffery SS (2012) Multiplex molecular analysis of CTCs. Recent Results Cancer Res 195:125–140. doi:10.1007/978-3-642-28160-0_11

Stott SL, Hsu CH, Tsukrov DI, Yu M, Miyamoto DT, Waltman BA, Rothenberg SM, Shah AM, Smas ME, Korir GK, Floyd FP Jr, Gilman AJ, Lord JB, Winokur D, Springer S, Irimia D, Nagrath S, Sequist LV, Lee RJ, Isselbacher KJ, Maheswaran S, Haber DA, Toner M (2010a) Isolation of circulating tumor cells using a microvortex-generating herringbone-chip. Proc Natl Acad Sci USA 107(43):18392–18397. doi:10.1073/pnas.1012539107

Stott SL, Lee RJ, Nagrath S, Yu M, Miyamoto DT, Ulkus L, Inserra EJ, Ulman M, Springer S, Nakamura Z, Moore AL, Tsukrov DI, Kempner ME, Dahl DM, Wu CL, Iafrate AJ, Smith MR, Tompkins RG, Sequist LV, Toner M, Haber DA, Maheswaran S (2010b) Isolation and characterization of circulating tumor cells from patients with localized and metastatic prostate cancer. Sci Transl Med 2(25):25ra23. doi:10.1126/scitranslmed.3000403

van de Stolpe A, Pantel K, Sleijfer S, Terstappen LW, den Toonder JM (2011) Circulating tumor cell isolation and diagnostics: toward routine clinical use. Cancer Res 71(18):5955–5960. doi:10.1158/0008-5472.CAN-11-1254

Voldman J (2006) Electrical forces for microscale cell manipulation. Annu Rev Biomed Eng 8:425–454. doi:10.1146/annurev.bioeng.8.061505.095739

Zetter BR (1998) Angiogenesis and tumor metastasis. Annu Rev Med 49:407–424. doi:10.1146/annurev.med.49.1.407

Zheng S, Lin HK, Lu B, Williams A, Datar R, Cote RJ, Tai YC (2011) 3D microfilter device for viable circulating tumor cell (CTC) enrichment from blood. Biomed Microdevices 13(1): 203–213. doi:10.1007/s10544-010-9485-3